Low Loss and Low Dispersion Fiber for Transmission Applications in the Terahertz Regime

Sohel Rana, Adnan Siraj Rakin, Harish Subbaraman, *Member, IEEE*,
Rainer Leonhardt, and Derek Abbott, *Fellow, IEEE*

***Abstract*— In this letter, we present a novel slotted core fiber incorporating a slotted cladding for the terahertz band. The modal properties of the designed fiber are numerically investigated based on an efficient finite element method. Simulation results of the fiber exhibit both a low material absorption loss of 0.0103–0.0145 cm^{-1} and low dispersion below 0.5 ps/THz/cm within the 0.5–0.9 THz range. In addition, a number of other features of the fiber have been evaluated.**

***Index Terms*— Far-infrared or terahertz, microstructures fibers, effective material loss, polymers, waveguide dispersion.**

I. Introduction

TERAHERTZ optical fibers are a significant area of research due to a number of potential application areas. This promising frequency range lies between 0.1–10 THz, and is a bridge between the microwave and optical bands [1]. Evidence of its wide range of application is seen in fields such as sensing [2], biotechnology [3], imaging [4]–[6], spectroscopy [7], communication [8], astronomy [9], non-invasive imaging [10] etc. However, most dielectric materials demonstrate extremely high material loss in this frequency range. Additionally, most present terahertz systems still depend on free space propagation. As a consequence, a number of attempts to improve material loss and dispersion in the terahertz band have been carried out [11]–[12].

In order to overcome the hurdles associated with terahertz technology in a practical optical communication system, different types of fiber design have been proposed. Dry air is a loss-less material but the mode field expands outside of waveguide if a dielectric waveguide is bounded by dry air [13] and this can result in a high bending loss. Using circular air holes in a porous fiber designed by [1] gave rise to reduced loss and a flat dispersion waveguide for terahertz propagation from 0.98 to 1.15 THz. About the same time, authors in [14] reported an octagonal porous fiber and the effective material loss (EML) findings of the design was 0.076 cm^{-1} at 1 THz. In 2014, Imran et al. [15] suggested a similar structure to that presented by [14] and was able reduce the EML further. Here, cyclic-olefin copolymer with the trade name TOPAS was used as the fiber material with a core porosity of 61.76% and a core diameter of 390 μm suggested for optimum design. This porous core fiber resulted in an ultra low absorption loss of 0.056 cm^{-1} and near zero flat dispersion in the 1.0–1.8 THz frequency range. Based on the same TOPAS material a rotated porous core hexagonal fiber was implemented that resulted in an EML of 0.066 cm^{-1} [16]. Later, a highly birefringent porous-core PCF was designed by exploiting dual asymmetry of the structure [17]; the fiber design reduced fabrication difficulties by utilizing circular air-holes [18]. The latest development shows that dual-hole units can be introduced into the fiber core for attaining low loss and high birefringence [19]. Again, the EML was reduced by 29% [20] whereas previous work in this field resulted in higher loss [14]. A kagome structure [21] exhibited a low absorption loss of 0.035 cm^{-1} and variation of dispersion of 0.61 $\pm$ 0.14 ps/THz/cm. Two recent hybrid designs demonstrated an improvement in EML of 0.037 cm^{-1} [22] and 0.019 cm^{-1} [23], and dispersion coefficients of 0.40 $\pm$ 0.04 ps/THz/cm [22] and 0.95 $\pm$ 0.05 ps/THz/cm [23], respectively. All of the designs reported still suffer relatively large EML and high dispersion that is undesirable for all terahertz applications.

In this letter, for the first time, we report a slotted-core photonic crystal fiber (PCF) incorporating a slotted cladding. The proposed fiber exhibits not only low EML but also low dispersion. Slotted fibers with air-cladding [24], [25] circular lattice cladding [26] and kagome cladding [27] were reported earlier.

II. Design Principle

In this work, a new design is presented with the objective to decrease the effective material loss. The geometry of the designed rectangular slotted porous fiber is depicted in Fig. 1. The outside diameter of the waveguide is 3.64 mm. The design exploits a slotted core that is surrounded by a slotted structure. The fiber consists of seven rectangular slots in the core and another twelve in the cladding. Different lengths for the slots of the cladding were chosen whereas the lengths of the slots in the core are all the same. The length of the slots immediately above and below the core in the cladding region are L =3.2 mm. The two outermost slots have a length of $0.4L$ and $0.7L$. Slots with length of $0.44L$ are positioned left and right sides of the core in the cladding structure while the

Manuscript received February 24, 2017; revised March 21, 2017; accepted April 7, 2017. Date of publication April 12, 2017; date of current version April 26, 2017. *(Corresponding author: Sohel Rana.)*

S. Rana and H. Subbaraman are with the Department of Electrical and Computer Engineering, Boise State University, Boise, ID 83725 USA (e-mail: dsmsrana@gmail.com; harishsubbaraman@boisestate.edu).

A. S. Rakin is with the Department of Electrical and Electronic Engineering, Bangladesh University of Engineering and Technology, Dhaka 1000, Bangladesh (e-mail: adnanrakin@gmail.com).

R. Leonhardt is with the Department of Physics, University of Auckland, Auckland 1010, New Zealand (e-mail: r.leonhardt@auckland.ac.nz).

D. Abbott is with the School of Electrical and Electronic Engineering, University of Adelaide, Adelaide, SA 5005, Australia (e-mail: derek.abbott@adelaide.edu.au).

Color versions of one or more of the figures in this letter are available online at http://ieeexplore.ieee.org.

Digital Object Identifier 10.1109/LPT.2017.2693203

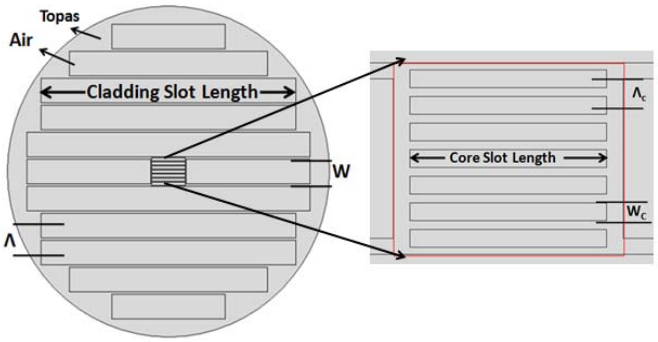

Fig. 1. Geometric structure of the fiber.

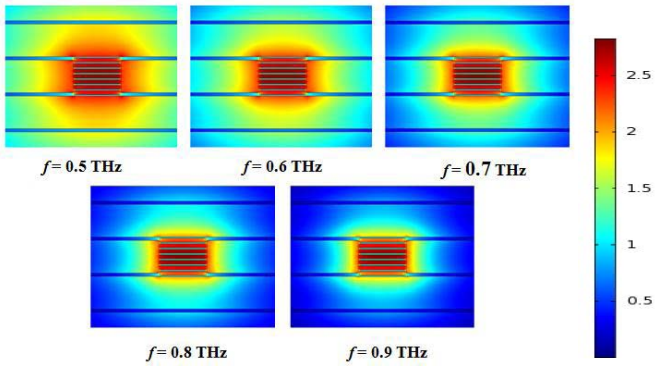

Fig. 2. Distribution of $E(y)$-field within the proposed fiber at various frequencies (linear scale for the field).

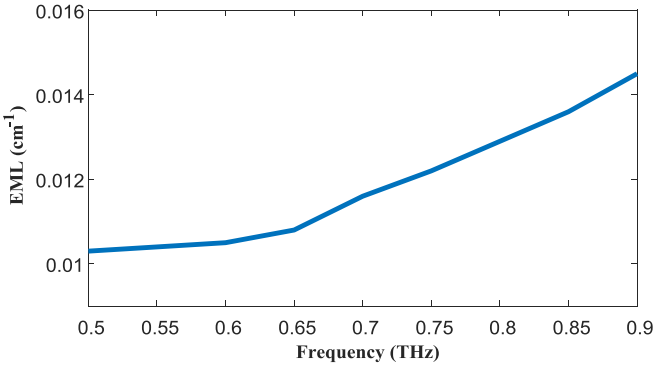

Fig. 3. Behaviour of EML with respect to frequency.

rest of the slots have length of $0.9L$. Additionally, all the slots in the cladding region have a width of 0.27 mm. Every slot in the core has a length of $0.12L$ and a width of $0.01L$. The center-to-center distance of two adjacent slots is called pitch, and is indicated by Λ_c and Λ for the core and the cladding, respectively. The width of the cladding and the core slots are denoted by W and W_C respectively.

Extending the length of the slots in the core would further reduce the EML. However, considering the implications for fabrication, the distance between the core slots and the cladding slots is kept constant at a value of 0.01 mm.

A number of dielectric materials have been used as a fiber material for broadband applications [28]–[30]. However, TOPAS has been selected as the bulk material for the presented fiber for its excellent inherent characteristics such as a constant refractive index of $n = 1.53$ in the 0.1–2 THz range [31], very low bulk material absorption loss of 0.2 cm^{-1} at $f = 1$ THz [32] insensitivity to humidity [33], and the fact that it is suited for biosensing [34]. Due to the low filling fraction in most areas of the waveguide the choice of material is not critical, i.e. other materials such as HDPE may be suitable as well.

III. Numerical Results and Discussion

To calculate the guiding properties of the proposed fiber, the finite element method (FEM) based on COMSOL software is used. A circular perfectly matched layer boundary is used to model the leakage properties. The diameter of this boundary is 4 mm.

The distribution of the $E(y)$-field within the fiber is shown in Fig. 2 for different terahertz frequencies. Here we show the fundamental mode polarized in the vertically direction. At 0.5 THz the effective refractive index for this mode is 1.023. Due to the asymmetry of the design, the waveguide will be birefringent and therefore the effective refractive index for the fundamental mode polarized horizontally is slightly different with $n_{\text{eff}}(h) = 1.060$. The simulations indicate that other modes can exist in the waveguide structure but for these other modes most of the intensity is propagating in the cladding and not the core. So when a focussed, fundamental Gaussian beam is launched at the centre of the waveguide, only the fundamental modes will be excited, and the waveguide will show single-mode characteristics. Figure 2 also unveils that tight confinement occurs at higher frequency and therefore less light escapes the core.

Analysis of the absorption loss is first investigated with the aid of an analytical expression. In order to characterize the loss of a terahertz waveguide, the effective material loss (EML) parameter has been introduced [35]

$$\alpha_{\text{eff}} = \sqrt{\frac{\varepsilon_0}{\mu_0}}\left(\frac{\int_{\text{mat}} \text{n}_{\text{mat}} |\text{E}|^2 \alpha_{\text{mat}} \text{dA}}{\left|\int_{\text{all}} \text{S}_\text{z} \text{dA}\right|}\right) \tag{1}$$

where n_{mat} is the refractive index, α_{mat} is the material absorption loss (in our case for TOPAS), ε_{o} is the permittivity and μ_{o} is the permeability of vacuum, E is the mode distribution of the E-field, and S_z is the Poynting vector in the z direction.

Effective material loss of the proposed waveguide at various frequencies is shown in Fig. 3. Within the frequency range 0.5–0.9 THz the proposed fiber shows ultralow EML between 0.0103–0.0145cm^{-1}, which is only between 4.9% and 7.3% of the bulk material loss of the background material. The EML results of this fiber are clearly lower than previously reported values for other designs [14]–[27]. Investigation of the EML of the terahertz radiation in Fig. 3 unveils that the EML increases slightly with frequency, and this is explained by the fact that stronger confinement occurs for smaller wavelengths and that the core contains a slightly larger percentage of the bulk material.

The percentage of transmitted power within the slotted core of the proposed fiber is also investigated. The fraction of transmitted power can be calculated using previously developed

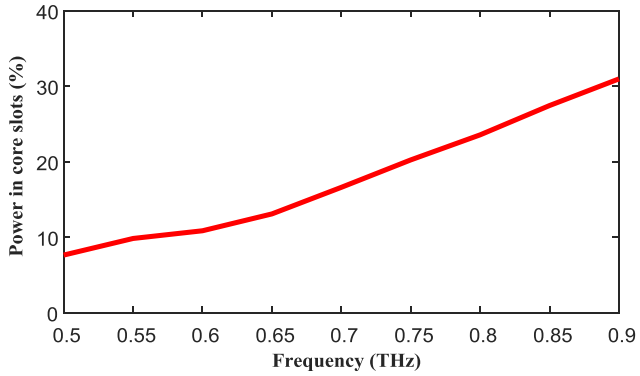

Fig. 4. Fraction of guided power within the core slots versus frequency.

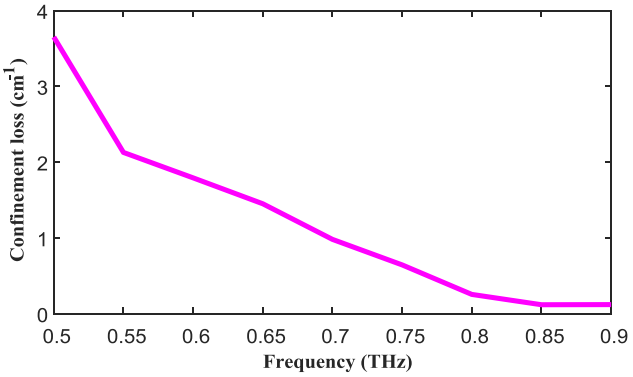

Fig. 5. Confinement loss versus frequency.

equation [37]

$$\eta' = \frac{\int_X S_z dA}{\int_{all} S_z dA}. \tag{2}$$

The behaviour of the power fraction that propagates within the core is shown in Fig. 4 where it is observed that even for high frequencies only a moderate amount, about 31% of the the power, is transmitted within the slotted air-holes. It is possible to increase this power fraction by increasing the width of the slots. However, that will reduce the refractive index difference between the cladding and the core, and delocalize most of the transmitted power into the cladding thereby incurring additional leakage loss.

Limitation due to the finite size of the air slots in the cladding causes another kind of loss that is called confinement loss, and that can be evaluated by [36]

$$\alpha_{CL} = 8.686 \frac{2\pi f}{c} \mathrm{Im}(n_{eff}) \times 10^{-2} \mathrm{dB/cm} \tag{3}$$

where c and f are the velocity of light in free space and the frequency of the light respectively, and $\mathrm{Im}(n_{eff})$ is the imaginary part of the complex refractive index.

From Fig. 5 it is clearly seen that the confinement loss as a function of the frequency decays rapidly toward higher frequencies. The reason behind this behaviour is that higher frequencies (i.e. smaller wavelengths) are confined more tightly as shown previously, and this results in a low confinement loss.

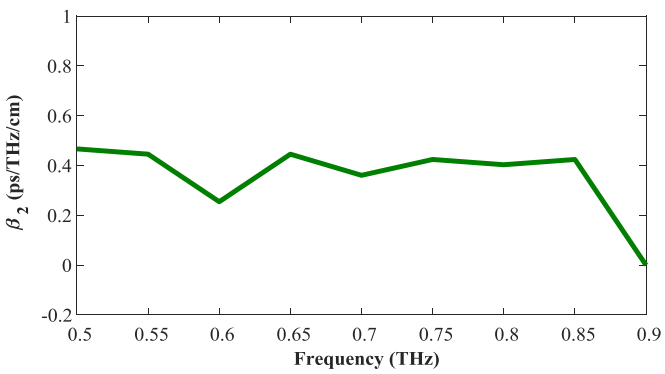

Fig. 6. Frequency dependency of the waveguide dispersion.

Dispersion analysis adds another important characteristic to the novel fiber design. TOPAS has a constant refractive index within a frequency range of 0.1–2 THz [31], so it is expected that waveguide dispersion will be the major contributor, and this can be calculated with Equation 4 [37]

$$\beta_2 = \frac{2}{c}\frac{dn_{eff}}{d\omega} + \frac{\omega}{c}\frac{d^2 n_{eff}}{d\omega^2} \tag{4}$$

Figure 6 clearly indicates that within the entire frequency range from 0.5 THz to 0.9 THz, the proposed fiber exhibits a dispersion that is always less than 0.5 ps/THz/cm and therefore better than most of the previously reported porous core fibers in terahertz regime.

Present fabrication technology due to its excellent progress with PCF technology is certainly able to produce many complex designs. However, because of the rectangular slots, the fabrication of the proposed porous fiber may not be possible by stacking or drilling preforms. Microstructure fibers, which are not in circular shape and are made of polymers and soft glasses, are still feasible for fabrication by established extrusion techniques [38]. In 2009, an asymmetric porous fiber with rectangular slots was designed experimentally by Atakaramians et al. using this method [24]. They took the advantage of a two-step process to fabricate the polymer fibers. Therefore it is expected that it is possible to fabricate the proposed fiber using the proven methods described above.

IV. Conclusion

We have introduced a new type of very low EML fiber consisting of a slotted core and a slotted cladding. The mode of the fiber is tightly confined to the core. The design results in a record low loss for high frequencies and very low dispersion. Difficulties such as fabrication and related issues have also been discussed.

References

[1] J. Liang, L. Ren, N. Chen, and C. Zhou, "Broadband, low-loss, dispersion flattened porous core photonic bandgap fiber for terahertz (THz)-wave propagation," *Opt. Commun.*, vol. 295, pp. 257–261, May 2015.

[2] R. H. Jacobsen, D. M. Mittleman, and M. C. Nuss, "Chemical recognition of gases and gas mixtures with terahertz waves," *Opt. Lett.*, vol. 21, no. 24, pp. 2011–2013, Dec. 1996.

[3] M. Nagel, P. Haring Bolivar, M. Brucherseifer, H. Kurz, A. Bosserhoff, and R. Büttner, "Integrated THz technology for label-free genetic diagnostics," *Appl. Phys. Lett.*, vol. 80, no. 1, pp. 154–156, Jan. 2002.

[4] W. L. Chan, W. Lam, J. Deibel, and D. M. Mittleman, "Imaging with terahertz radiation," *Rep. Prog. Phys.*, vol. 70, no. 8, pp. 1325–1379, Jul. 2007.

[5] D. M. Mittleman, M. Gupta, R. Neelamani, R. G. Baraniuk, J. V. Rudd, and M. Koch, "Recent advances in terahertz imaging," *Appl. Phys.*, vol. 68, no. 6, pp. 1085–1094, Jun. 1999.

[6] H. T. Chen, R. Kersting, and G. C. Cho, "Terahertz imaging with nanometer resolution," *Appl. Phys. Lett.*, vol. 83, no. 15, pp. 3009–3011, Oct. 2003.

[7] J. Zhang and D. Grischkowsky, "Waveguide terahertz time-domain spectroscopy of nanometer water layers," *Opt. Lett.*, vol. 29, no. 14, pp. 1617–1619, Jul. 2004.

[8] D. Pinto and S. S. A. Obayya, "Improved complex-envelope alternating-direction-implicit finite-difference-time-domain method for photonic-bandgap cavities," *J. Lightw. Technol.*, vol. 25, no. 1, pp. 440–447, Jan. 2007.

[9] L. Ho, M. Pepper, and P. Taday, "Terahertz spectroscopy: Signatures and fingerprints," *Nature Photon*, vol. 2, no. 9, p. 541, Sep. 2008.

[10] Q. Chen, Z. Jiang, G. X. Xu, and X.-C. Zhang, "Near-field terahertz imaging with a dynamic aperture," *Opt. Lett.*, vol. 25, no. 15, pp. 1122–1124, 2000.

[11] R. Mendis and D. Grischkowsky, "THz interconnect with low-loss and low-group velocity dispersion," *IEEE Microw. Wireless Compon. Lett.*, vol. 11, no. 11, pp. 444–446, Nov. 2001.

[12] H. Han, H. Park, M. Cho, and J. Kim, "Terahertz pulse propagation in a plastic photonic crystal fiber," *Appl. Phys. Lett.*, vol. 80, no. 15, pp. 2634–2636, 2002.

[13] L.-J. Chen, H.-W. Chen, T.-F. Kao, J.-Y. Lu, and C.-K. Sun, "Low-loss subwavelength plastic fiber for terahertz waveguiding," *Opt. Lett.*, vol. 31, no. 3, pp. 308–310, 2006.

[14] S. F. Kaijage, Z. Ouyang, and X. Jin, "Porous-core photonic crystal fiber for low loss terahertz wave guiding," *IEEE Photon. Technol. Lett.*, vol. 25, no. 15, pp. 1454–1457, Aug. 1, 2013.

[15] I. Hasan, S. M. A. Razzak, G. K. M. Hasanuzzaman, and S. Habib, "Ultra-low material loss and dispersion flattened fiber for THz transmission," *IEEE Photon. Technol. Lett.*, vol. 26, no. 23, pp. 2372–2375, Dec. 1, 2014.

[16] R. Islam, G. K. M. Hasanuzzaman, M. S. Habib, S. Rana, and M. A. G. Khan, "Low-loss rotated porous core hexagonal single-mode fiber in THz regime," *Opt. Fiber Technol.*, vol. 24, pp. 38–43, Aug. 2015.

[17] R. Islam, M. S. Habib, G. K. M. Hasanuzzaman, S. Rana, and M. A. Sadath, "Novel porous fiber based on dual-asymmetry for low-loss polarization maintaining THz wave guidance," *Opt. Lett.*, vol. 41, no. 3, pp. 440–443, Feb. 2014.

[18] T. E. Y. Wang, H. Jiang, Z. Hu, and K. Xie, "High birefringence photonic crystal fiber with high nonlinearity and low confinement loss," *Opt. Exp.*, vol. 23, no. 7, pp. 8329–8337, Apr. 2015.

[19] G. K. M. Hasanuzzaman, S. Rana, and M. S. Habib, "A novel low loss, highly birefringent photonic crystal fiber in THz regime," *IEEE Photon. Technol. Lett.*, vol. 28, no. 8, pp. 899–902, Apr. 15, 2016.

[20] S. Rana, G. K. M. Hasanuzzaman, S. Habib, S. F. Kaijage, and R. Islam, "Proposal for a low loss porous core octagonal photonic crystal fiber for T-ray wave guiding," *Opt. Eng.*, vol. 53, no. 11, p. 115107, 2014.

[21] G. K. M. Hasanuzzaman *et al.*, "Low loss single-mode porous-core kagome photonic crystal fiber for THz wave guidance," *J. Lightw. Technol.*, vol. 33, no. 19, pp. 4027–4031, Oct. 1, 2015.

[22] S. Ali, N. Ahmed, S. Aljunid, and B. Ahmad, "Ultra-flat low material loss porous core THz waveguide with near zero flat dispersion," *Electron. Lett.*, vol. 52, no. 10, pp. 863–865, 2016.

[23] S. Ali, N. Ahmed, S. Aljunid, and B. Ahmad, "Hybrid porous core low loss dispersion flattened fiber for THz propagation," *Photon. Nanostruct.-FundamAppl.*, vol. 22, pp. 18–23, Nov. 2016.

[24] S. Atakaramians *et al.*, "THz porous fibers: Design, fabrication and experimental characterization," *Opt. Exp.*, vol. 17, no. 16, pp. 14053–14062, Jul. 2009.

[25] S. Atakaramians, S. A. Vahid, B. M. Fischer, D. Abbott, and T. M. Monro, "Low loss, low dispersion and highly birefringent terahertz porous fibers," *Opt. Commun.*, vol. 282, no. 1, pp. 36–38, 2009.

[26] R. Islam, M. S. Habib, G. K. M. Hasanuzzaman, R. Ahmad, S. Rana, and S. F. Kaijage, "Extremely high-birefringent asymmetric slotted-core photonic crystal fiber in THz regime," *IEEE Photon. Technol. Lett.*, vol. 27, no. 21, pp. 2222–2225, Nov. 1, 2015.

[27] M. R. Hasan, M. S. Anower, M. S. Hasan, and S. M. A. Razzak, "Polarization maintaining low-loss slotted core kagome lattice THz fiber," *IEEE Photon. Technol. Lett.*, vol. 28, no. 16, pp. 1751–1754, Aug. 15, 2016.

[28] R. Yahiaoui, H. Němec, P. Kužel, F. Kadlec, C. Kadlec, and P. Mounaix, "Tunable THz metamaterials based on an array of paraelectric $SrTiO_3$ rods," *Appl. Phys. A, Solids Surf.*, vol. 103, no. 3, pp. 689–692, 2011.

[29] R. Yahiaoui, H. Němec, P. Kužel, F. Kadlec, C. Kadlec, and P. Mounaix, "Broadband dielectric terahertz metamaterials with negative permeability," *Opt. Lett.*, vol. 34, no. 22, pp. 3541–3543, Nov. 2009.

[30] H. Němec, P. Kužel, F. Kadlec, C. Kadlec, R. Yahiaoui, and P. Mounaix, "Tunable terahertz metamaterials with negative permeability," *Phys. Rev. B, Condens. Matter*, vol. 79, no. 24, p. 241108, 2009.

[31] H. Bao, K. Nielsen, H. K. Rasmussen, P. U. Jepsen, and O. Bang, "Fabrication and characterization of porous-core honeycomb bandgap THz fibers," *Opt. Exp.*, vol. 20, no. 28, pp. 29507–29517, Dec. 2012.

[32] K. Nielsen, H. K. Rasmussen, A. J. L. Adam, P. C. M. Planken, O. Bang, and P. U. Jepsen, "Bendable, low-loss Topas fibers for the terahertz frequency range," *Opt. Exp.*, vol. 17, no. 10, pp. 8592–8601, May 2009.

[33] W. Yuan *et al.*, "Humidity insensitive TOPAS polymer fiber Bragggrating sensor," *Opt. Exp.*, vol. 19, no. 20, pp. 19731–19739, Sep. 2011.

[34] G. Emiliyanov, P. E. Høiby, L. H. Pedersen, and O. Bang, "Selective serial multi-antibody biosensing with TOPAS microstructured polymer optical fibers," *Sensors*, vol. 13, no. 3, pp. 3242–3251, Mar. 2013.

[35] K. Nielsen, H. K. Rasmussen, P. U. Jepsen, and O. Bang, "Porous-core honeycomb bandgap THz fiber," *Opt. Lett.*, vol. 36, no. 5, pp. 666–668, Mar. 2011.

[36] S. Rana, M. S. Islam, M. Faisal, K. C. Roy, R. Islam, and S. F. Kaijage, "Single-mode porous fiber for low-loss polarization maintaining terahertz transmission," *Opt. Eng.*, vol. 55, no. 7, p. 076114, Jul. 2016.

[37] J. Liang, L. Ren, N. Chen, and C. Zhou, "Broadband, low-loss, dispersion flattened porous-core photonic bandgap fiber for terahertz (THz)-wave propagation," *Opt. Commun.*, vol. 295, pp. 257–261, May 2013.

[38] H. Ebendorff-Heidepriem and T. M. Monro, "Extrusion of complex preforms for microstructured optical fibers," *Opt. Exp.*, vol. 15, no. 23, pp. 15086–15092, Nov. 2007.